the FEBS Journal

# Template-assisted rational design of peptide inhibitors of furin using the lysine fragment of the mung bean trypsin inhibitor

Hu Tao[1,2,*], Zhen Zhang[2,*], Jiahao Shi[1], Xiao-xia Shao[2], Dafu Cui[1] and Cheng-wu Chi[1,2]

1 Institute of Biochemistry and Cell Biology, Shanghai Institutes for Biological Sciences, Graduate School of the Chinese Academy of Sciences, The Chinese Academy of Sciences, Shanghai, China
2 Institute of Protein Research, Tongji University, Shanghai, China

**Keywords**
furin; kexin; molecular design; mung bean trypsin inhibitor; peptide synthesis

**Correspondence**
C. Chi, Shanghai Institute of Biochemistry and Cell Biology, Chinese Academy of Sciences, 320 Yue Yang Road, Shanghai 200031, China
Fax: +86 21 54921011
Tel: +86 21 54921165
E-mail: chi@sunm.shcnc.ac.cn

*These authors contributed equally to this work

(Received 24 March 2006, revised 30 May 2006, accepted 23 June 2006)

doi:10.1111/j.1742-4658.2006.05393.x

Highly active, small-molecule furin inhibitors are attractive drug candidates to fend off bacterial exotoxins and viral infection. Based on the 22-residue, active Lys fragment of the mung bean trypsin inhibitor, a series of furin inhibitors were designed and synthesized, and their inhibitory activity towards furin and kexin was evaluated using enzyme kinetic analysis. The most potent inhibitor, containing 16 amino acid residues with a $K_i$ value of $2.45 \times 10^{-9}$ M for furin and of $5.60 \times 10^{-7}$ M for kexin, was designed with three incremental approaches. First, two nonessential Cys residues in the Lys fragment were deleted via a Cys-to-Ser mutation to minimize peptide misfolding. Second, residues in the reactive site of the inhibitor were replaced by the consensus substrate recognition sequence of furin, namely, Arg at $P_1$, Lys at $P_2$, Arg at $P_4$ and Arg at $P_6$. In addition, the $P_7$ residue Asp was substituted with Ala to avoid possible electrostatic interference with furin inhibition. Finally, the extra N-terminal and C-terminal residues beyond the doubly conjugated disulfide loops were further truncated. However, all resultant synthetic peptides were found to be temporary inhibitors of furin and kexin during a prolonged incubation, with the scissile peptide bond between $P_1$ and $P_1'$ being cleaved to different extents by the enzymes. To enhance proteolytic resistance, the $P_1'$ residue Ser was mutated to D-Ser or *N*-methyl-Ser. The *N*-methyl-Ser mutant gave rise to a $K_i$ value of $4.70 \times 10^{-8}$ M for furin, and retained over 80% inhibitory activity even after a 3 h incubation with the enzyme. By contrast, the D-Ser mutant was resistant to cleavage, although its inhibitory activity against furin drastically decreased. Our findings identify a useful template for the design of potent, specific and stable peptide inhibitors of furin, shedding light on the molecular determinants that dictate the inhibition of furin and kexin.

Furin, a member of the family of proprotein convertases found in mammalian cells, is a membrane-associated, calcium-dependent serine endoprotease that specifically cleaves the peptide bond after paired basic amino acid residues in substrates such as growth factors, receptors, serum proteins, coagulation factors and extracellular matrix proteins [1–6]. Ubiquitously expressed at low levels within the trans-Golgi

**Abbreviations**
$\alpha_1$-PDX, $\alpha_1$-antitrypsin Portland; Acm, acetamidomethyl; Bzl, benzyl; cHex, cyclohexyl; ClZ, chlorobenzyloxycarbonyl; HOBt, *N*-hydroxybenzotriazole; MBTI, mung bean trypsin inhibitor; MCA, amino-4-methylcoumarin; 4-Meb, 4-methylbenzyl; Pam, phenylacetamidomethyl; Pbf, 2,2,4,6,7-pentamethyldihydrobenzofuran-5-sulfonyl; 2-PDS, 2-dithiodipyridine; SFTI-1, sunflower trypsin inhibitor-1; TAME, tosylarginine methyl ester; tBu, t-butyl; Tos, tosyl; Trt, trityl.

network/endosomal system [7,8], furin is also essential for the activation of bacterial exotoxins such as diphtheria toxin and anthrax toxin, and for the processing of viral envelope glycoproteins of HIV and SARS virus [9–12]. As expected, furin inhibitors have been shown to be able to neutralize bacterial exotoxins and prevent viral infection [13]. Therefore, much recent work has been aimed at designing various peptide-based or protein-based furin inhibitors, including the peptidyl inhibitor decanoyl-Arg-Val-Lys-Arg-$CH_2Cl$ [14], bioengineered variants of $\alpha_1$-antitrypsin Portland ($\alpha_1$-PDX) [15], polyarginines [16], *Drosophila* serpin 4 [17,18], eglin C [19,20], the serpin-derived peptides, and the barley serine proteinase inhibitor 2-derived cyclic peptides [21].

Our previous studies identified the mung bean trypsin inhibitor (MBTI), composed of 72 amino acid residues and seven disulfide bonds, as a member of the Bowman–Birk protease inhibitor family [22]. MBTI forms a symmetric structure consisting of two domains, both with an antitrypsin reactive site – one located at Lys20–Ser21 (in the Lys domain) and the other at Arg47–Ser48 (in the Arg domain). Active Lys and Arg domains can be separated from each other by limited peptic digestion and purified on an immobilized trypsin affinity column at different pH values [23]. Since the inhibitory activity of the Lys domain was higher than that of the Arg domain, this study focused on the former. The Lys domain consists of two peptide chains, which are composed of 26 and nine residues, respectively, and connected by two interchain disulfide bonds. A 22-residue synthetic peptide derived from the long chain with three intramolecular disulfide bonds remained active against trypsin (Fig. 1A), and two disulfide isoforms of this peptide inhibited the enzyme with $K_i$ values of $1.2 \times 10^{-7}$ M and $4 \times 10^{-8}$ M [24].

A backbone-cyclized, potent trypsin inhibitor, sunflower trypsin inhibitor-1 (SFTI-1), of 14 amino acid residues belonging to the Bowman–Birk family was identified from sunflower [25]. SFTI-1 comprises a canonical, reactive site disulfide loop of nine amino acid residues commonly found in the Bowman–Birk family of inhibitors. The disulfide loop in SFTI-1 differs from that in the Lys domain of MBTI by only one noncontact residue at position 10, numbering from the N-terminal Gly of SFTI-1, where it is Ile in SFTI-1 and Gln in MBTI (Fig. 1B,C) [26]. The remaining five residues in SFTI-1 form a backbone-cyclized ring structure instead of a second disulfide loop, as found in other Bowman–Birk inhibitors. Not surprisingly, the sunflower trypsin inhibitor and the Lys fragment of MBTI adopt the same conformation in the nine-residue reactive site loop region, as shown in the crystal structures of their complexes with trypsin [24,26].

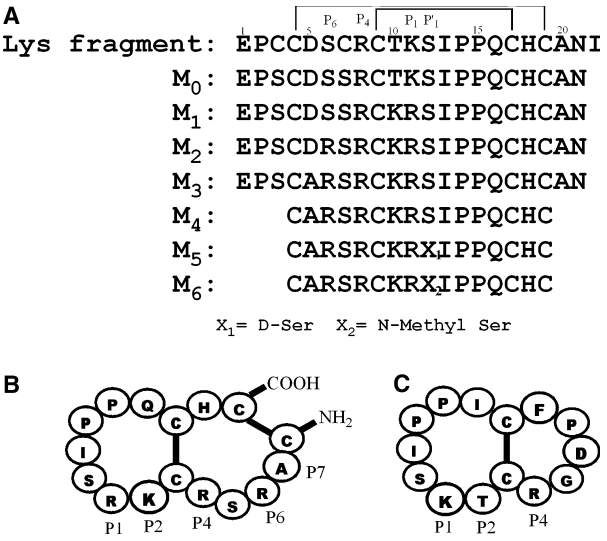


**Fig. 1.** (A) The amino acid sequences of the previously synthesized Lys fragment [24] and its mutants studied in this work. (B,C) The topologic structures of the $M_4$ variant of the mung bean trypsin inhibitor (MBTI) Lys fragment and sunflower trypsin inhibitor-1 (SFTI-1).

Small-molecule peptide inhibitors of proteases are attractive lead compounds for therapeutic development because of their potency, specificity, low toxicity and cost-effectiveness. SFTI-1, as one of the smallest peptide-based natural trypsin inhibitors, has shown significant potential to be used as a template molecule for the design of specific inhibitors to target biomedically important enzymes. Owing to its small size and strong inhibitory activity against trypsin, the Lys fragment of MBTI may also serve as an ideal template for the design of potent, specific and stable furin inhibitors. Here we report the design and synthesis of various peptide analogs derived from the Lys fragment of MBTI and their functional characterization with respect to furin and kexin.

## Results and Discussion

### Optimization of the Lys fragment template

There are six cysteine residues in the 22-residue Lys fragment of MBTI (Fig. 1A). The Cys9–Cys17 pair, forming the canonical, nine-residue reactive site loop, is indispensable for inhibitory activity. The Cys4–Cys19 pair, forming a second nine-residue loop in support of the adjacent reactive site loop, is important for maintaining a stable peptide conformation. On the other

**Table 1.** Molecular masses and inhibitory constants of the synthetic peptides on furin, kexin and trypsin.

| | $M_r$ | | $K_i$ | | |
|---|---|---|---|---|---|
| Mutants | Theoretical | Determined | Furin (M) | Kexin (M) | Trypsin (M) |
| $M_0$ | 2259.53 | 2259.2 | $2.48 \pm 0.05 \times 10^{-6}$ | $> 10^{-5}$ | $6.36 \pm 1.65 \times 10^{-9}$ |
| $M_1$ | 2314.61 | 2314.5 | $3.53 \pm 0.31 \times 10^{-8}$ | $2.58 \pm 0.12 \times 10^{-6}$ | $> 10^{-4}$ |
| $M_2$ | 2383.72 | 2383.2 | $6.21 \pm 0.29 \times 10^{-9}$ | $1.54 \pm 0.04 \times 10^{-6}$ | $> 10^{-4}$ |
| $M_3$ | 2339.71 | 2339.5 | $3.26 \pm 0.02 \times 10^{-9}$ | $4.75 \pm 0.01 \times 10^{-7}$ | $> 10^{-4}$ |
| $M_4$ | 1841.21 | 1841.6 | $2.45 \pm 0.28 \times 10^{-9}$ | $5.60 \pm 0.31 \times 10^{-7}$ | $> 10^{-4}$ |
| $M_5$ | 1841.21 | 1841.4 | $2.43 \pm 0.11 \times 10^{-5}$ | $3.53 \pm 0.03 \times 10^{-7}$ | $> 10^{-4}$ |
| $M_6$ | 1855.23 | 1855.6 | $4.70 \pm 0.06 \times 10^{-8}$ | $2.01 \pm 0.20 \times 10^{-7}$ | $> 10^{-4}$ |

hand, Cys3 and Cys7 disulfide bonded with two corresponding Cys residues from the Arg domain in native MBTI appear to be nonessential both structurally and functionally in the context of the Lys fragment [23]. We showed in our previous work that oxidation of a synthetic Lys fragment resulted in two active isoforms with $K_i$ values of $4 \times 10^{-8}$ M and $1.2 \times 10^{-7}$ M [24]. It is plausible that the canonical disulfide loop was intact in both isoforms and that isomerization resulted from multiple disulfide connectivities afforded by Cys3, Cys7, Cys4 and Cys19. Therefore, the first step in optimizing the Lys fragment template was to replace Cys3 and Cys7 by Ser in order to avoid unnecessary disulfide mispairing. The resultant peptide with two conjugated nine-residue loops, termed $M_0$, did indeed exhibit higher inhibitory activity against trypsin ($K_i$ $6.36 \times 10^{-9}$ M) than the two previously characterized disulfide isoforms of the Lys fragment (Table 1).

The second step was to introduce into the reactive site of the Lys template the consensus substrate recognition sequence of furin. Both furin and kexin are highly specific for Arg at $P_1$ and prefer basic residues at $P_2$ and $P_4$ [6,27–30]. In contrast to kexin, however, furin also prefers basic residues at $P_6$ and is able to recognize residues at even more distant sites [6,31]. The stringent specificity of furin and kexin has been explained by their crystal structures [32–34], in which electrostatic forces dominating subsite interactions in enzyme–inhibitor or enzyme–substrate complexes appear to be a specificity determinant.

The $M_0$ construct already contains Lys at $P_1$ and Arg at $P_4$, and thus meets the minimal requirement as a furin or kexin inhibitor. In fact, the $M_0$ peptide displayed a modest inhibitory activity against furin and kexin, with $K_i$ values of $2.48 \times 10^{-6}$ M and $> 10^{-5}$ M, respectively. Replacement of the residues at the $P_2$ and $P_1$ sites in $M_0$ by Lys and Arg, respectively, resulted in $M_1$. The $K_i$ of $M_1$ for furin, i.e. $3.53 \times 10^{-8}$ M, decreased by two orders of magnitude compared with that of $M_0$, in accord with the previous finding that the Lys($P_2$)–Arg($P_1$) combination is preferred for furin inhibition [31]. When Ser6 in $M_1$ was substituted with Arg, the inhibitory activity of the resultant $M_2$ against furin further increased by five-fold, but to a much less extent against kexin, indicating that a basic residue at the $P_6$ site is desirable for furin, but less important for kexin. Interestingly, when Asp7 in $M_2$ was replaced by Ala, the inhibitory activity of the resultant $M_3$ peptide against both furin and kexin further improved by 2–3-fold, suggesting that a negatively charged residue at $P_7$ is functionally deleterious, possibly due to electrostatic interference with subsite interactions involving the neighboring Arg at $P_6$.

The final step was to remove the N-terminal Glu-Pro-Ser and C-terminal Ala-Asn residues flanking Cys4 and Cys19 in $M_3$. The truncation at both termini apparently had no negative impact on the inhibitory activity of $M_4$ against the enzymes, resulting in a miniaturized (16 residues) and potent furin inhibitor ($K_i$ $2.45 \times 10^{-9}$ M) derived from the 22-residue Lys fragment of MBTI.

It is worth pointing out that both $M_4$ (Fig. 1B) and the sunflower trypsin inhibitor (Fig. 1C) have the same topologic structure, containing an active canonical nine-residue loop and a conjugated disulfide loop in $M_4$ or a backbone-cyclized loop in SFTI-1.

## Temporary inhibition

When the synthetic analogs ($M_0$ to $M_4$) were incubated with furin, their inhibitory activity gradually decreased in a time-dependent fashion. $M_4$ appeared to be most stable, with more than 60% activity remaining after 3 h, whereas the least stable $M_0$ lost more than 60% activity during the same period of time. Similar results were also observed with kexin. Notably, the higher the $K_i$ value, the faster the activity decayed (Fig. 2). These findings indicate that synthetic inhibitors were progressively hydrolyzed, probably at the reactive site, by the enzyme during prolonged incubation. An $M_4$ cleaved

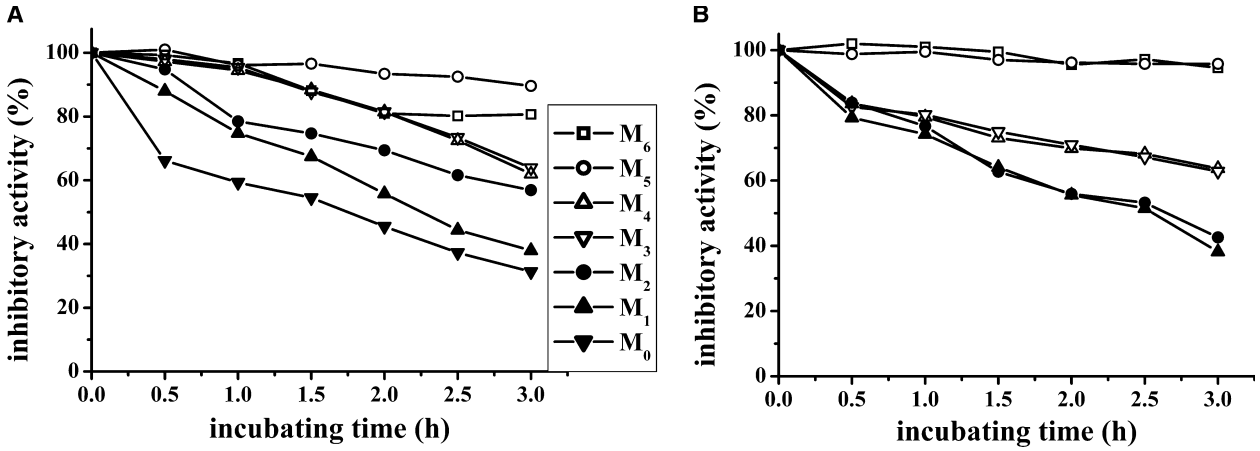


**Fig. 2.** Stability of the mutants during incubation with furin (A) and kexin (B). The inhibitory activities of the mutants were determined at different time intervals.

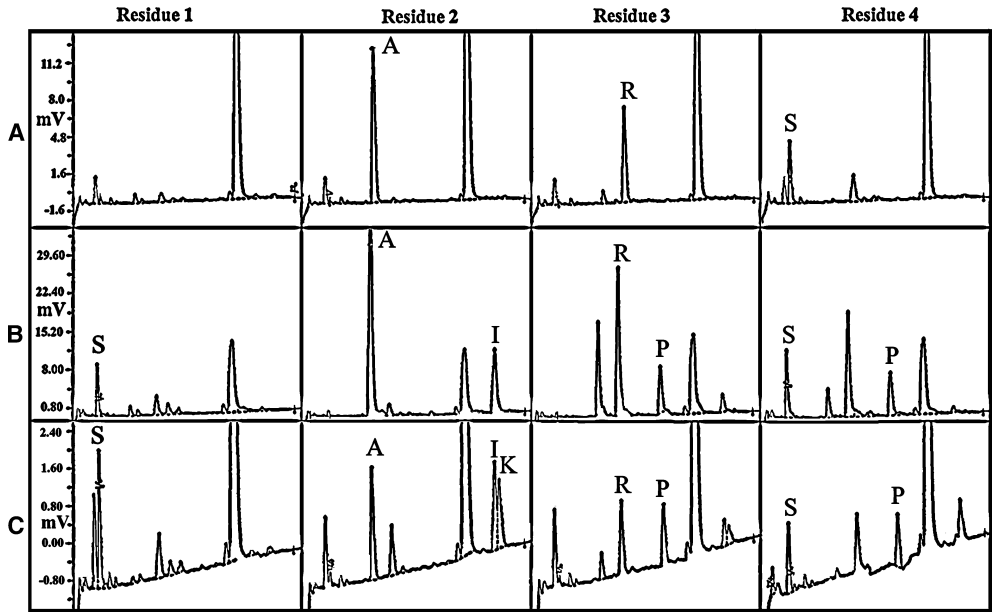


**Fig. 3.** Identification of the cleavage sites of $M_4$ by N-terminal sequencing. (A) Edman degradation of $M_4$. One nmol of $M_4$ was used for sequencing. The N-terminal residue Cys was not detected during Edman degradation, as it was paired with another C-terminal Cys. The detected sequence then started from the second N-terminal residue. (B) $M_4$ after incubation with furin. A suitable amount of furin was incubated with 10 μL of 1 mM $M_4$ in 1 mL of 100 mM Hepes buffer, pH 7.5, containing 1 mM $CaCl_2$, 0.5% Triton X-100 and 1 mM β-mercaptoethanol at 37 °C for 3 h. After being desalted on a Sephadex G10 column, the hydrolyzed peptide was used for Edman sequencing as described above. (C) $M_4$ after incubation with trypsin. One microgram of trypsin was incubated with 10 μL of 1 mM $M_4$ in 1 mL of 20 mM Tris/HCl buffer, pH 7.8, containing 10 mM $CaCl_2$, at 25 °C for 5 min. Twenty microliters of the reaction mixture was added to the sequencing membrane, washed twice with 500 μL of water to remove the salt, and fixed in the cartridge for Edman sequencing.

by furin was purified and sequenced, and the results indeed confirmed the hydrolysis of the $P_1$–$P_1'$ peptide bond (Fig. 3).

Numerous studies suggest that conformational rigidity in the reactive site loop region of a peptide/protein inhibitor of proteases is a key to proteolytic resistance. Destabilization of the reactive site loop invariably converts an otherwise strong inhibitor to a good substrate for the same enzyme. In many protease inhibitors, conformational rigidity in the reactive site loop region is partially provided by a side-chain–side-chain interaction between $P_2$ and $P_1'$ residues. This is clearly

the case for the Lys fragment of MBTI, where the $O^{\gamma 1}$ atom of $P_2$ Thr is H-bonded to the $O^{\gamma}$ atom of $P_1'$ Ser [35]. In fact, Thr is considered to be the optimal residue at the $P_2$ site for Bowman–Birk inhibitors [36]. Thus, it is not surprising that the Thr-to-Lys mutation at $P_2$ converted $M_0$ from a strong trypsin inhibitor ($K_i$ $6.36 \times 10^{-9}$ M) to a series of weak and temporary ones ($M_1$ to $M_4$), with $K_i$ values over $10^{-4}$ M. Sequence analysis of cleavage products indicated that two peptide bonds in the $M_1$ to $M_4$ analogs were cleaved during incubation with trypsin, one located between $P_4$ and $P_3$ (Arg–Cys) and the other between $P_1$ and $P_1'$ (Arg–Ser) (Fig. 3C). It is highly plausible that in the designed furin inhibitors ($M_1$ to $M_4$) with a $P_2$ Lys, the absence of a $P_2$–$P_1'$ side-chain interaction is detrimental to their proteolytic resistance to furin.

### Construction of a stable furin inhibitor

Incorporation of unnatural amino acids into peptides has been widely used in the design of protease-resistant peptide mimetics [37]. Since D-amino acids are not recognized by naturally occurring proteases, replacement of enzyme-susceptible residues by D-amino acids can eliminate proteolytic degradation by both exoproteases and endoproteases. Many other options are available to tackle proteolysis by changing only the peptide bond structure, leaving the side-chain untouched, including, but not limited to, N-methylation, i.e. –CON($CH_3$)–, peptoid structures, i.e. –[N(R)–$CH_2$–CO]*n*–, and β-amino acids [37]. Based on the optimized $M_4$ template, the $P_1'$ residue Ser was further mutated in order to construct a stable furin inhibitor. The $P_1'$ Ser was replaced by D-Ser or *N*-methyl-Ser, resulting in $M_5$ and $M_6$, respectively. As expected, the Arg–D-Ser peptide bond in $M_5$ was resistant to cleavage. However, the inhibitory activity of $M_5$ against furin, due to steric incomplementarity in the enzyme–inhibitor complex, drastically decreased by four orders of magnitude, with a $K_i$ value of $2.43 \times 10^{-5}$ M. By contrast, $M_6$ remained a potent inhibitor against furin ($K_i$ $4.70 \times 10^{-8}$ M) and largely resistant to proteolysis, with over 80% inhibitory activity preserved even after a 3 h incubation with furin (Fig. 2). It is worth pointing out that, compared with $M_4$, both $M_5$ and $M_6$ showed similar inhibitory activity against kexin, indicating that the $P_1'$ site residue is not critical for the interaction with the enzyme.

## Conclusions

We have demonstrated through a series of incremental modifications to the Lys fragment of MBTI that a potent furin inhibitor can be designed. Further improvement is possible through a refined sequence–activity study to enhance its activity, specificity and stability. In light of its small size and high potency, the $M_6$ template may serve as an ideal lead compound for the development of furin inhibitor-based therapeutics for the treatment of infectious diseases. Our designed furin inhibitor may also provide a useful tool for better understanding the molecular basis for the activity and specificity of furin, and for designing peptide inhibitors to target other members of the proprotein convertase family as well.

## Experimental procedures

### Materials

All Boc and Fmoc amino acids were obtained from Applied Biosystems, Foster City, CA, USA. Boc-Asn-phenylacetamidomethyl (Pam) resin, Boc-Cys [acetamidomethyl (Acm)]-Pam resin and Fmoc-Cys [trityl (Trt)] hydroxymethylphenoxymethyl polystyrene resin were obtained from PE (Rockford, IL). The purified furin was a gift from I. Lindberg (Louisiana State University). The gene encoding prokexin was a gift from R.S. Fuller (University of Michigan Medical School) [20].

### Peptide synthesis

Peptides were synthesized by solid-phase peptide synthesis using a 430A peptide synthesizer (Applied Biosystems) and the *N*,*N*′-dicyclohexylcarbodiimide (DCC1)/*N*-hydroxybenzotriazole (HOBt) method. The protected amino acids are: Glu [O-cyclohexyl (cHex)], Asp (O-cHex; Boc-L-glutamic acid 5-cyclohexyl ester), Ser [benzyl (Bzl)], Cys [4-methylbenzyl (4-Meb); Acm], Lys [chlorobenzyloxycarbonyl (ClZ)], Arg [tosyl (Tos)] and Thr (Bzl). The 4-Meb protecting group was used for residues Cys9 and Cys17 of the essential canonical loop of peptides $M_0$, $M_1$, $M_2$, $M_3$ and $M_4$. The Acm protecting group was used for the remaining two cysteine residues of all peptides. Boc-amino acids were activated with equivalent amounts of *N*,*N*′-dicyclohexylcarbodiimide and HOBt. Each coupling reaction was carried out with a four-fold excess of activated Boc-amino acid for the first time and with an equivalent amount of activated Boc-amino acid for the next two times. After the final cycle, the peptide was cleaved from the resin by HF containing 5% *p*-cresol and a few drops of phenol and thioanisole used as a scavenger to remove free radicals generated during the reaction for 80 min at 0 °C. After removal of the HF, the product was washed with ethyl acetate and extracted with 0.1% trifluoroacetic acid containing 20% acetonitrile. The extract was lyophilized. All protecting groups except Acm of the crude peptide were removed by the HF cleavage.

The Fmoc solid-phase synthesis of peptides $M_5$ and $M_6$ was performed in an ABI 433 peptide synthesizer starting from Fmoc-Cys [trityl (Trt)] hydroxymethylphenoxymethyl polystyrene resin. The protected amino acids are: Fmoc-Arg [2,2,4,6,7-pentamethyldihydrobenzofuran-5-sulfonyl (Pbf)], Fmoc-Lys (Boc), Fmoc-D-Ser [t-butyl (tBu)], Fmoc-*N*-methyl-Ser (tBu), Fmoc-Cys (Trt, Acm), Fmoc-His (Trt) and Fmoc-Glu (Trt). The Trt protecting group was used for Cys1 and Cys16, and the Acm protecting group was used for Cys9 and Cys17. The resin was cleaved by trifluoroacetic acid containing 5% *p*-cresol and a few drops of triethylsilane and thioanisole for 1 h at room temperature. After removal of trifluoroacetic acid, the product was washed with diethyl ether and extracted with 0.1% trifluoroacetic acid containing 20% acetonitrile. The extract was lyophilized to obtain the crude product with Acm groups unremoved.

## Reduction and selective oxidation of disulfide bonds

For selective oxidation of disulfide bonds, different protecting groups were used for the cysteine residues in Boc and Fmoc solid-phase synthesis, namely, HF-labile 4-Meb and HF-stable Acm in the Boc method, and trifluoroacetic acid-labile Trt and trifluoroacetic acid-stable Acm in the Fmoc method. After cleavage by HF in the Boc method, the deprotected cysteines were oxidized by 2-dithiodipyridine (2-PDS) to form the first disulfide bond (canonical loop) [38], the Acm protecting groups of two other cysteine residues were removed by iodine/oxygen, and the deprotected cysteine residues were oxidized to form another disulfide bond (conjugated loop). In Fmoc peptide synthesis, the Trt protecting group was used for the first pair of cysteine residues (conjugated loop), and Acm for another pair (canonical loop).

The crude peptide (12 mg) synthesized by the Boc method or the Fmoc method was dissolved in 6 mL of 8 M urea containing a 50-fold amount of dithiothreitol. After flushing with nitrogen, the solution in the stoppered tube was incubated at 37 °C for 3 h. The reduced peptide solution was desalted on a Sephadex G15 column (Amersham Biosciences, Piscataway, NJ, USA), washed with 0.1% trifluoroacetic acid, lyophilized, and dissolved in 1 mL of 0.1% trifluoroacetic acid. The reduced peptide solution was added to 100 mL of 20 mM, pH 6, sodium acetate buffer, and 0.15 mM 2-PDS [38] in 10% methanol was dropped in, the molar ratio of peptide to 2-PDS being 1 : 0.9. The peptide solution was oxidized for 18 h and lyophilized. After being desalted on a Sephadex G15 column and purified by HPLC, the remaining Acm-protected cysteines were further deprotected. One milligram of purified peptide was added to 10 mL of acetonitrile containing 1% trifluoroacetic acid and 14.5 mM $I_2$, the molar ratio of the peptide to $I_2$ being 1 : 5. The two disulfide bonds were then correctly paired, and the peptide was purified on a Zorbax $C_{18}$ column (10 × 250 mm) (Agilent, Palo Alto, CA, USA) equilibrated with buffer A (0.1% trifluoroacetic acid in water) at a flow rate of 2 mL·min$^{-1}$. The peptide was eluted with a stepwise gradient: 0–20% buffer B (70% acetonitrile in 0.8% trifluoroacetic acid) for 5 min, and 20–40% buffer B for 30 min. The molecular masses of all synthetic peptides determined with an ABI API2000 Q-trap mass spectroscope were consistent with their theoretical values, as shown in Table 1.

## Inhibition kinetic analysis for furin and kexin

The enzyme activity of furin and kexin was measured at 37 °C in a final volume of 1 mL of Hepes buffer (100 mM, pH 7.5, 1 mM $CaCl_2$, 0.5% Triton X-100, and 1 mM β-mercaptoethanol) containing different amounts of the fluorogenic amino-4-methylcoumarin (MCA) substrate (pyrArg-Thr-Lys-Arg-MCA). For each assay, an equivalent amount of enzyme was added to release 15 nmol of MCA in the 1 min enzyme reaction. For determination of the inhibitory activity, a fixed amount of enzyme was first incubated with different amounts of the inhibitor at 37 °C for 5 min, and the residual enzyme activity was measured with an F-4500 fluorescence spectrophotometer (Hitachi, Tokyo, Japan). The incubation time needed for equilibrium to be reached between enzyme and inhibitor was estimated to be less than 5 min, as all initial velocities were the same up to 30 min of incubation. The excitation and emission wavelengths were 370 nm and 460 nm, respectively. The $K_i$ values for furin or kexin were measured by Dixon's plot ($1/V$ against $I$) using different concentrations of substrate (50 and 80 μM for furin, 10 and 15 μM for kexin) [39]. Data from three measurements were averaged, and linear regression analysis and standard errors were calculated using the ORIGIN program to obtain the equilibrium inhibition constant $K_i$.

## Inhibition kinetic analysis for trypsin

The inhibitory activities of the synthetic peptides toward trypsin were measured at 25 °C, using the substrate tosyl-arginine methyl ester (TAME). One microgram of trypsin (Sigma-Aldrich, St Louis, MO, USA) was first incubated for 5 min with different amounts of the inhibitor in 1 mL of 20 mM Tris/HCl (pH 7.8) buffer containing 10 mM $CaCl_2$, and TAME was added to a final concentration of 160 and 320 μM. The increase in absorbance was immediately measured at 247 nm. The same method as described above was used for $K_i$ determination.

## N-terminal sequencing

Amino acid sequencing was performed by automated Edman degradation using a Perkin-Elmer Applied Biosys-

tems 494 pulsed-liquid phase protein sequencer (Procise) with an on-line 785A PTH-amino acid analyzer.

## Acknowledgements

We would like to thank Dr R. S. Fuller for the full-length gene of prokexin and Dr I. Lindberg for the purified recombinant mouse furin. We also would like to thank Drs Wuyuan Lu, Youshang Zhang and Jinbo Han for helpful discussions.

## References

1 Brennan SO & Nakayama K (1994) Furin has the proalbumin substrate specificity and serpin inhibitory properties of an in situ hepatic convertase. *FEBS Lett* **338**, 147–151.
2 Bresnahan PA, Leduc R, Thomas L, Thorner J, Gibson HL, Brake AJ, Barr PJ & Thomas G (1990) Human fur gene encodes a yeast KEX2-like endoprotease that cleaves pro-beta-NGF in vivo. *J Cell Biol* **111**, 2851–2859.
3 Mondino A, Giordano S & Comoglio PM (1991) Defective posttranslational processing activates the tyrosine kinase encoded by the MET proto-oncogene (hepatocyte growth factor receptor). *Mol Cell Biol* **11**, 6084–6092.
4 Pei D & Weiss SJ (1995) Furin-dependent intracellular activation of the human stromelysin-3 zymogen. *Nature* **375**, 244–247.
5 Wasley LC, Rehemtulla A, Bristol JA & Kaufman RJ (1993) PACE/furin can process the vitamin K-dependent pro-factor IX precursor within the secretory pathway. *J Biol Chem* **268**, 8458–8465.
6 Rockwell NC, Krysan DJ, Komiyama T & Fuller RS (2002) Precursor processing by kex2/furin proteases. *Chem Rev* **102**, 4525–4548.
7 Thomas G (2002) Furin at the cutting edge: from protein traffic to embryogenesis and disease. *Nat Rev Mol Cell Biol* **3**, 753–766.
8 Anderson ED, Molloy SS, Jean F, Fei H, Shimamura S & Thomas G (2002) The ordered and compartment-specfic autoproteolytic removal of the furin intramolecular chaperone is required for enzyme activation. *J Biol Chem* **277**, 12879–12890.
9 Tsuneoka M, Nakayama K, Hatsuzawa K, Komada M, Kitamura N & Mekada E (1993) Evidence for involvement of furin in cleavage and activation of diphtheria toxin. *J Biol Chem* **268**, 26461–26465.
10 Klimpel KR, Molloy SS, Thomas G & Leppla SH (1992) Anthrax toxin protective antigen is activated by a cell surface protease with the sequence specificity and catalytic properties of furin. *Proc Natl Acad Sci USA* **89**, 10277–10281.
11 Hallenberger S, Bosch V, Angliker H, Shaw E, Klenk HD & Garten W (1992) Inhibition of furin-mediated cleavage activation of HIV-1 glycoprotein gp160. *Nature* **360**, 358–361.
12 Bergeron E, Vincent MJ, Wickham L, Hamelin J, Basak A, Nichol ST, Chretien M & Seidah NG (2005) Implication of proprotein convertases in the processing and spread of severe acute respiratory syndrome coronavirus. *Biochem Biophys Res Commun* **326**, 554–563.
13 Moehring JM, Inocencio NM, Robertson BJ & Moehring TJ (1993) Expression of mouse furin in a Chinese hamster cell resistant to Pseudomonas exotoxin A and viruses complements the genetic lesion. *J Biol Chem* **268**, 2590–2594.
14 Garten W, Hallenberger S, Ortmann D, Schafer W, Vey M, Angliker H, Shaw E & Klenk HD (1994) Processing of viral glycoproteins by the subtilisin-like endoprotease furin and its inhibition by specific peptidylchloroalkylketones. *Biochimie* **76**, 217–225.
15 Jean F, Stella K, Thomas L, Liu G, Xiang Y, Reason AJ & Thomas G (1998) alpha1-Antitrypsin Portland, a bioengineered serpin highly selective for furin: application as an antipathogenic agent. *Proc Natl Acad Sci USA* **95**, 7293–7298.
16 Cameron A, Appel J, Houghten RA & Lindberg I (2000) Polyarginines are potent furin inhibitors. *J Biol Chem* **275**, 36741–36749.
17 Oley M, Letzel MC & Ragg H (2004) Inhibition of furin by serpin Spn4A from Drosophila melanogaster. *FEBS Lett* **577**, 165–169.
18 Osterwalder T, Kuhnen A, Leiserson WM, Kim YS & Keshishian H (2004) Drosophila serpin 4 functions as a neuroserpin-like inhibitor of subtilisin-like proprotein convertases. *J Neurosci* **24**, 5482–5491.
19 Komiyama T & Fuller RS (2000) Engineered eglin c variants inhibit yeast and human proprotein processing proteases, Kex2 and furin. *Biochemistry* **39**, 15156–15165.
20 Liu ZX, Fei H & Chi CW (2004) Two engineered eglin c mutants potently and selectively inhibiting kexin or furin. *FEBS Lett* **556**, 116–120.
21 Villemure M, Fournier A, Gauthier D, Rabah N, Wilkes BC & Lazure C (2003) Barley serine proteinase inhibitor 2-derived cyclic peptides as potent and selective inhibitors of convertases PC1/3 and furin. *Biochemistry* **42**, 9659–9668.
22 Zhang YS, Lo SS, Tan FL & Chi CW (1982) Complete amino acid sequence of mung bean trypsin inhibitor. *Sci Sinica Ser B* **25**, 268–277.
23 Zhu Y, Huang Q & Chi C (1999) Crystal structure of mung bean inhibitor lysine active fragment complex with bovine beta-trypsin at 1.8A resolution. *J Biomol Struct Dyn* **16**, 1219–1224.
24 Li Y, Huang Q, Zhang S, Liu S, Chi C & Tang Y (1994) Studies on an artificial trypsin inhibitor peptide

derived from the mung bean trypsin inhibitor: chemical synthesis, refolding, and crystallographic analysis of its complex with trypsin. *J Biochem (Tokyo)* **116**, 18–25.

25 Korsinczky ML, Schirra HJ, Rosengren KJ, West J, Condie BA, Otvos L, Anderson MA & Craik DJ (2001) Solution structures by 1H NMR of the novel cyclic trypsin inhibitor SFTI-1 from sunflower seeds and an acyclic permutant. *J Mol Biol* **311**, 579–591.

26 Luckett S, Garcia RS, Barker JJ, Konarev AV, Shewry PR, Clarke AR & Brady RL (1999) High-resolution structure of a potent, cyclic proteinase inhibitor from sunflower seeds. *J Mol Biol* **290**, 525–533.

27 Rockwell NC & Fuller RS (1998) Interplay between S1 and S4 subsites in Kex2 protease: Kex2 exhibits dual specificity for the P4 side chain. *Biochemistry* **37**, 3386–3391.

28 Rockwell NC, Wang GT, Krafft GA & Fuller RS (1997) Internally consistent libraries of fluorogenic substrates demonstrate that Kex2 protease specificity is generated by multiple mechanisms. *Biochemistry* **36**, 1912–1917.

29 Brenner C & Fuller RS (1992) Structural and enzymatic characterization of a purified prohormone-processing enzyme: secreted, soluble Kex2 protease. *Proc Natl Acad Sci USA* **89**, 922–926.

30 Nakayama K (1997) Furin: a mammalian subtilisin/Kex2p-like endoprotease involved in processing of a wide variety of precursor proteins. *Biochem J* **327**, 625–635.

31 Krysan DJ, Rockwell NC & Fuller RS (1999) Quantitative characterization of furin specificity. Energetics of substrate discrimination using an internally consistent set of hexapeptidyl methylcoumarinamides. *J Biol Chem* **274**, 23229–23234.

32 Henrich S, Cameron A, Bourenkov GP, Kiefersauer R, Huber R, Lindberg I, Bode W & Than ME (2003) The crystal structure of the proprotein processing proteinase furin explains its stringent specificity. *Nat Struct Biol* **10**, 520–526.

33 Holyoak T, Wilson MA, Fenn TD, Kettner CA, Petsko GA, Fuller RS & Ringe D (2003) 2.4 A resolution crystal structure of the prototypical hormone-processing protease Kex2 in complex with an Ala-Lys-Arg boronic acid inhibitor. *Biochemistry* **42**, 6709–6718.

34 Henrich S, Lindberg I, Bode W & Than ME (2005) Proprotein convertase models based on the crystal structures of furin and kexin: explanation of their specificity. *J Mol Biol* **345**, 211–227.

35 Song HK, Kim YS, Yang JK, Moon J, Lee JY & Suh SW (1999) Crystal structure of a 16 kDa double-headed Bowman–Birk trypsin inhibitor from barley seeds at 1.9 A resolution. *J Mol Biol* **293**, 1133–1144.

36 Gariani T & Leatherbarrow RJ (1997) Stability of protease inhibitors based on the Bowman–Birk reactive site loop to hydrolysis by proteases. *J Pept Res* **49**, 467–475.

37 Cardillo G, Gentilucci L & Tolomelli A (2006) Unusual amino acids: synthesis and introduction into naturally occurring peptides and biologically active analogues. *Mini Rev Med Chem* **6**, 293–304.

38 Maruyama K, Nagasawa H & Suzuki A (1999) 2,2′-Bispyridyl disulfide rapidly induces intramolecular disulfide bonds in peptides. *Peptides* **20**, 881–884.

39 Dixon M (1953) The determination of enzyme inhibitor constants. *Biochem J* **55**, 170–171.